

WW AND WZ PRODUCTION AT THE TEVATRON

E. LIPELES

University of California, San Diego
E-mail: lipeles@fnal.gov

This report summarizes recent measurements of the production properties of WW and WZ pairs of bosons at the Tevatron. This includes measurements of the cross-section and triple gauge couplings in the WW process and the first evidence for WZ production.

Keywords: Diboson; WW ; WZ

1. Introduction

Boson pair production is one of the few processes that have significant effects from triple boson vertices at tree level. These couplings are predicted in the standard model and are directly related to its gauge group structure. One of the goals of diboson measurements is to limit deviations from the standard model values of these triple gauge couplings (TGCs). Such deviations could be observed in either the cross-sections or in the kinematic distributions of the observed events. Possible causes of anomalous TGCs include new particles in loop diagrams.¹ It is also possible for diboson final states to receive contributions from the s -channel production of an as yet unobserved particle, most notably the standard model Higgs decaying to a pair of W bosons.

This report summarizes recent measurements by the CDF and DØ collaborations of WW and WZ production at the Tevatron. The Tevatron produces $p\bar{p}$ collision at 1.96 TeV center of mass energy. The dominant contributions to the cross-sections for WW and WZ production are the t -channel (and similar u -channel) process involving two instances of the well measured boson-quark couplings and the s -channel process involving triple gauge couplings, shown in Figure 1. The TGCs can in general be functions of the invariant mass of the final state bosons $\sqrt{\hat{s}}$,

so measurements at the Tevatron complement previous measurements at LEP because they probe larger values of $\sqrt{\hat{s}}$. Furthermore, the WZ final state, which is not accessible in e^+e^- collisions, isolates the WWZ coupling from $WW\gamma$.

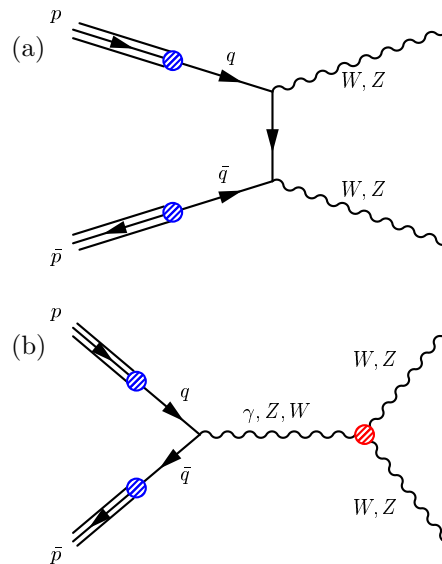


Fig. 1. Dominant diagrams in the production of boson pairs: (a) t -channel (b) s -channel.

Of the heavy diboson processes, WW production is the largest with a standard model next-to-leading order (NLO) prediction of $\sigma(WW)_{NLO} = 12.4 \pm 0.8$ pb, followed by WZ production with an NLO prediction of $\sigma(WZ)_{NLO} = 3.7 \pm 0.1$ pb.² Sec-

tion 2 of this report covers measurements of the WW cross-section; Section 3 describes measurements of the triple gauge couplings in WW production, and Section 4 presents the first evidence for WZ production.

2. WW cross-section

Both CDF and DØ have measured the WW production cross-section in the all leptonic final state $lv'l'\nu$, where $l, l' = e$ or μ . Although this is the lowest branching fraction final state of WW decay (4.6%), it has significantly lower backgrounds than the other final states, which all involve hadronic jets. The presence of neutrinos is identified as lack momentum balance in the plane transverse to the beam using the missing transverse energy variable $\cancel{E}_T \equiv \sum_i E_i \hat{n}_T^i$, where \hat{n}_T^i is the transverse component of a unit vector connecting the interaction point to a calorimeter cell i and E_i is the energy deposition in that cell. DØ requires $\cancel{E}_T \equiv |\vec{\cancel{E}}_T| > 30(ee), 40(\mu\mu), 20(e\mu)$ GeV while CDF requires $\cancel{E}_T > 25$ GeV for all final states.

The primary backgrounds to the $ll'\cancel{E}_T$ final state are from $W \rightarrow l\nu$ with an associated jet or photon which is misidentified as another lepton, Drell-Yan (Z/γ^*) production of lepton pairs combined with large false \cancel{E}_T due to detector effects, $t\bar{t} \rightarrow WWbb \rightarrow ll'\nu\nu bb$, and other heavy dibosons, either $WZ \rightarrow ll\nu\nu$, with a lost lepton, or $ZZ \rightarrow ll\nu\nu$. The predicted composition of the selected sample in the CDF analysis is shown in Table 1.

After selection of events with two leptons, significant \cancel{E}_T and a jet veto to suppress the $t\bar{t}$ background, CDF observes 95 events in 825 pb^{-1} of data with an expected background of $37.8 \pm 0.9(\text{stat.}) \pm 4.7(\text{syst.})^3$ and DØ observes 25 events in $224 - 252 \text{ pb}^{-1}$ of data with an expected background of $8.1 \pm 0.6(\text{stat}) \pm 0.6(\text{sys}) \pm 0.5(\text{lumi})^4$. These observations correspond to cross-sections of $\sigma(WW) = 13.6 \pm 2.3(\text{stat}) \pm 1.6(\text{sys}) \pm$

Table 1. Expected composition and observed yield for the CDF WW analysis.

Mode	Events \pm Stat \pm Syst
Drell-Yan	$11.8 \pm 0.8 \pm 3.1$
W +jets	$11.0 \pm 0.5 \pm 3.2$
$WZ + ZZ$	$7.9 \pm 0.0 \pm 0.8$
$W\gamma$	$6.8 \pm 0.2 \pm 1.4$
$t\bar{t}$	$0.2 \pm 0.0 \pm 0.0$
Sum Bkg	$37.8 \pm 0.9 \pm 4.7$
WW	$52.4 \pm 0.1 \pm 4.3$
Expected	$90.2 \pm 0.9 \pm 6.4$
Data	95

$1.2(lum)$ pb (CDF) and $\sigma(WW) = 13.8_{-3.8}^{+4.3}(\text{stat})_{-0.9}^{+1.2}(\text{sys}) \pm 0.9(lum)$ pb (DØ), both of which are consistent with a NLO calculation of the standard model expectation.

3. Triple gauge couplings in WW and WZ

The s -channel WW production process (shown in Figure 1b) has contributions from both $WW\gamma$ and WWZ TGCs while the WZ process only gets a contribution from the WWZ vertex. DØ has set limits on anomalous couplings in the $WW \rightarrow ll'\nu\nu$ sample described above.

CDF has recently probed the TGCs in the combination of WW and WZ modes using the $lvjj$ final state, where $l = e$ or μ . While the background in the $lvjj$ is dramatically larger than the purely leptonic final states due to the $p\bar{p} \rightarrow W$ +jets process, the branching fractions are ≈ 6.5 times higher for WW and ≈ 10 times higher for WZ . Because anomalous TGCs are expected to enhance the high W transverse momentum region, where the backgrounds from W +jets are smaller, the $lvjj$ final state can be sensitive to anomalous couplings even without observation of the standard model processes.

The TGCs are parameterized by adding terms with variable coupling constants to the

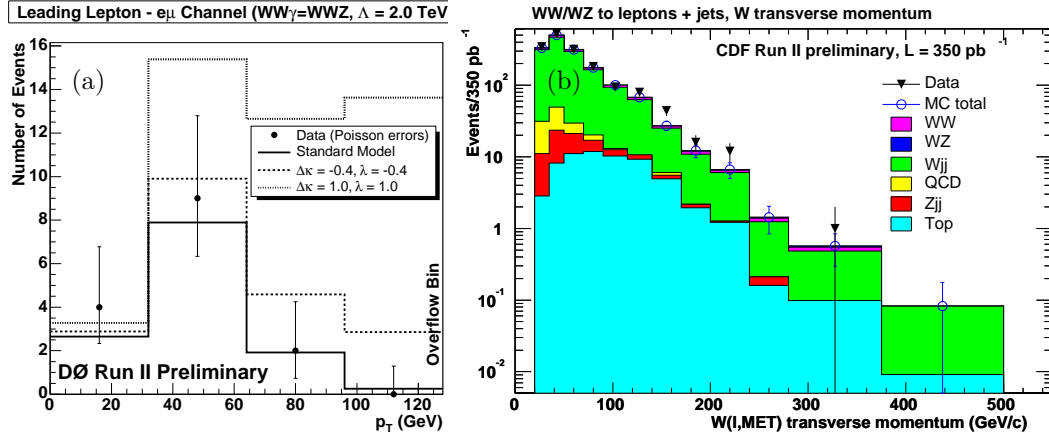


Fig. 2. Distributions which are fit for triple gauge couplings: (a) leading lepton p_T in the $ll'\nu\nu$ final state at D0 and (b) leptonically decaying W p_T in the $lvjj$ final state at CDF.

standard model Lagrangian

$$\mathcal{L}_{WWV} = ig_1^V (W_{\mu\nu} W^{\mu\nu} V^\nu - W_\mu V_\nu W^{\mu\nu}) + i\kappa_V W_\mu W_\nu V^{\mu\nu} + \frac{i\lambda_V}{M_W^2} W_{\lambda\mu} W_\nu^{\mu\nu} V^\lambda,$$

where $\kappa_\gamma = \kappa_Z = g_1^Z = 1$ and $\lambda_Z = \lambda_\gamma = 0$ in the standard model. These couplings can be related to the electric and magnetic dipole and quadrupole moments of the W and Z . In general the coupling constants $\alpha = \kappa_\gamma, \kappa_Z, g_1^Z, \lambda_Z$, and λ_γ can be functions of the invariant mass of the diboson pair $\sqrt{\hat{s}}$. As a simplification, both experiments assume the functional form $\alpha(\hat{s}) = \alpha_0 / (1 + \hat{s} / (2 \text{ TeV})^2)^2$, which turns off the couplings at very large \hat{s} where the couplings would violate unitarity. In order to further simplify the coupling parameter space, the equal coupling scheme is used, $\Delta\kappa \equiv \kappa_\gamma - 1 = \kappa_Z - 1$ and $\lambda \equiv \lambda_Z = \lambda_\gamma$ with $g_1^Z = 0$. Other simplifications of the parameter space have also been studied.

D0 sets limits on the anomalous coupling constants using the $ll'\nu\nu$ sample by fitting the leading lepton p_T spectrum as shown in Figure 2a). The figure shows the effect on the shape of the spectrum due to anomalous couplings near the current bounds. CDF performs a similar fit to the p_T spectrum of the leptonically decaying W in the $lvjj$ final state (Figure 2b). The results of these fits are

$$-0.32 < \Delta\kappa < 0.45 \text{ and } -0.29 < \lambda < 0.30 \text{ (D0)} \\ \text{and } -0.51 < \Delta\kappa < 0.44 \text{ and } -0.28 < \lambda < 0.28 \text{ (CDF).}$$

4. Search for WZ production

Both CDF and D0 search for WZ in the $ll'\nu\nu$ final state ($l, l' = e$ or μ) which has a combined branching fraction of 1.8%, including contributions from $\tau \rightarrow l\nu\nu$ where $l = e$ or μ . The small standard model prediction for the WZ cross-section makes this a very low rate signal, so both experiments have optimized their lepton selection criteria to maximize efficiency and acceptance.

The dominant backgrounds in these searches are $Z \rightarrow ll$ with a jet or photon misidentified as a lepton and $ZZ \rightarrow ll'l'$ where one lepton is not reconstructed. As shown in Figure 3, these backgrounds are both strongly suppressed by requiring the event to have $\cancel{E}_T > 25 \text{ GeV}$ (CDF), 20 GeV (D0).

CDF observes 2 events expecting $3.72 \pm 0.02(\text{stat.}) \pm 0.15(\text{syst.})$ WZ signal events and $0.92 \pm 0.07(\text{stat.})^{+0.16}_{-0.10}(\text{syst.})$ background events using 825 pb^{-1} of data. Based on this CDF sets an upper limit of $\sigma(WZ) < 6.3 \text{ pb}$ at 95% CL. D0 observes 12 events with an expectation of 7.5 ± 1.2

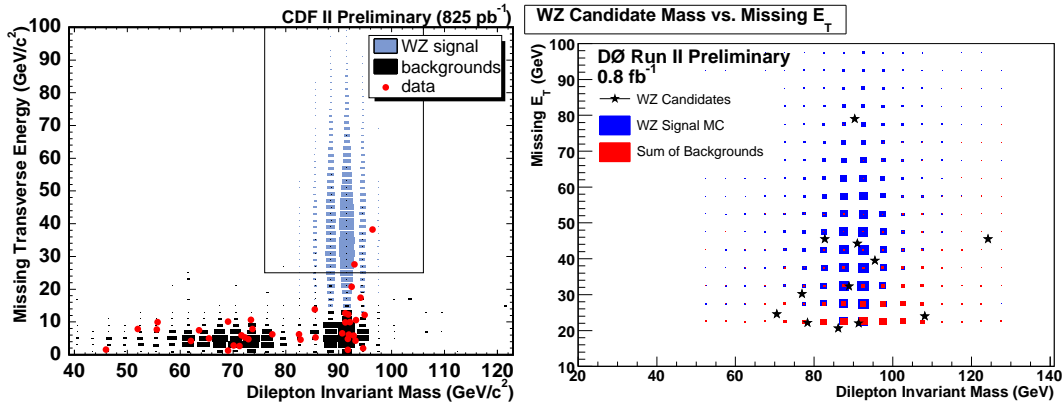


Fig. 4. The distributions of the observed events in the dilepton invariant mass versus \cancel{E}_T plane for (left) CDF and (right) DØ.

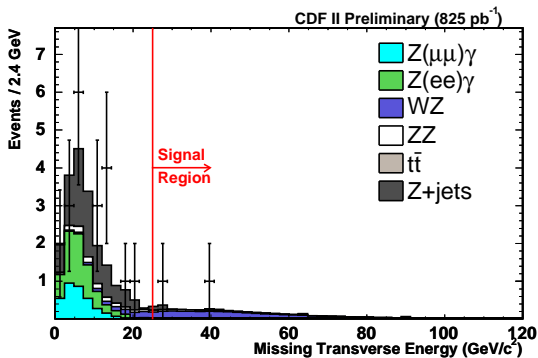


Fig. 3. The \cancel{E}_T distribution for $WZ \rightarrow ll'\nu$ candidate events at CDF showing the power of the \cancel{E}_T requirement for suppressing backgrounds.

signal and 3.6 ± 0.2 background events using 800 pb^{-1} of data. This constitutes 3.3σ evidence for WZ production and corresponds to a cross-section of $\sigma(WZ) = 4.0_{-1.5}^{+1.9} \text{ pb}$, consistent with the standard model prediction. The distributions of the observed events in the dilepton invariant mass versus \cancel{E}_T plane show that signal events cluster near the Z mass and values of \cancel{E}_T consistent with expectation (Figure 4).

5. Summary

With the increasingly large accumulated datasets at the Tevatron, CDF and DØ are probing electroweak diboson production with new sensitivity. Cross-section and triple

gauge coupling measurements for the WW final state are becoming increasingly precise, while the first evidence for WZ production has just been seen.

References

1. For a theoretical review of diboson physics at the Tevatron see: J. Ellison and J. Wudka, *Ann. Rev. Nucl. Part. Sci.* **48**, 33 (1998) [arXiv:hep-ph/9804322].
2. J. M. Campbell and R. K. Ellis, *Phys. Rev. D* **60**, 113006 (1999) [arXiv:hep-ph/9905386].
3. M. S. Neubauer [CDF Collaboration], arXiv:hep-ex/0605066.
4. V. M. Abazov *et al.* [DØ Collaboration], *Phys. Rev. Lett.* **94**, 151801 (2005), arXiv:hep-ex/0410066.
5. V. M. Abazov *et al.* [DØ Collaboration], arXiv:hep-ex/0608011.
6. V. M. Abazov *et al.* [DØ Collaboration], DØ Note 5110-CONF (available at <http://www-d0.fnal.gov>).